# Structural Dynamics of the Manganese-Stabilizing Protein—Effect of pH, Calcium, and Manganese†

Tatiana Shutova,‡,§ Julia Nikitina,‡,§ Gintaras Deikus,|| Bertil Andersson,‡,⊥ Vyacheslav Klimov,§ and Göran Samuelsson*,‡

*Umeå Plant Science Centre, Department of Plant Physiology, Umeå University, SE-901 87 Umeå, Sweden, Institute of Basic Biological Problems, Russian Academy of Sciences (RAS), 142290 Pushchino, Moscow, Russia, Department of Pharmacology and Biological Chemistry, Mount Sinai School of Medicine, New York University, New York, 10029, and Division of Cell Biology, Linköping University, SE-581 85 Linköping, Sweden*

*Received July 4, 2005; Revised Manuscript Received September 28, 2005*

ABSTRACT: The photosystem-II-associated 33-kDa extrinsic manganese-stabilizing protein is found in all oxygen-evolving organisms. In this paper, we show that this protein undergoes pH-induced conformational changes in the physiological pH range. At a neutral pH of 7.2, the hydrophobic amino acid residues that are most likely located inside the $\beta$ barrel are "closed" and the protein binds neither $Mn^{2+}$ nor $Ca^{2+}$ ions. When the protein is transferred to a solution with a slightly acidic pH of 5.7, hydrophobic amino acid residues become exposed to the surrounding medium, enabling them to bind the fluorescent probe 8,1-ANS. At this pH-induced open state, $Mn^{2+}$ and $Ca^{2+}$ bind to the manganese-stabilizing protein. The pH values used in this study, 7.2 and 5.7, are typical of the pH found in the thylakoid lumen in the dark and light, respectively. A model is presented in which the manganese-stabilizing protein undergoes a pH-dependent conformational change that in turn influences its capacity to bind calcium and manganese. In this model, the proton-dependent conformational changes of the tertiary structure of the manganese-stabilizing protein are of functional relevance for the regulation of substrate (water) delivery to and product (proton) release from the water-oxidizing complex by forming a proton-sensing proton-transport pathway.

Photosynthetic water oxidation takes place at a manganese-containing complex associated with photosystem II (PS II)[1] (*1*, *2*). In higher plants and cyanobacteria, at least six intrinsic proteins (D1, D2, CP47, CP43, and the two subunits of cytochrome b559) are required for the oxygen evolution activity (*3*). Furthermore, the extrinsic 33-kDa manganese-stabilizing protein (MSP) has been studied since its discovery 20 years ago with respect to a possible functional and/or structural role in PS II (see ref *4* for a review). The MSP, encoded by the psbO gene, is present in all known oxygenic phototrophs (*5*). Extraction of this protein from PS II particles by washing with a high concentration of $CaCl_2$ suppresses the oxygen evolution, but the manganese remains bound if the $Cl^-$ concentration is sufficiently high (*6*). At lower $Cl^-$ concentrations, two of the four manganese atoms are released from PS II (*7*). Removal of the MSP also affects the turnover and stability of the higher redox states of the water-oxidizing complex (WOC) (*8*). PS II, lacking the MSP evolves oxygen only at low rates, is susceptible to donor-side photoinhibition and requires nonphysiological levels of calcium and chloride ions for activity (*3*, *9*, *10*). Thus, the MSP is an important constituent of a fully intact WOC and essential for stabilization of the functional manganese cluster. As was shown recently, it is also involved in the regulation of water oxidation via GTP binding (*11*).

The 3.5 Å resolution X-ray crystal structure of a cyanobacterial PS II provides a detailed picture of MSP bound to the PS II core (*12*). The MSP faces the thylakoid lumen and is orientated at about a 40° angle relative to the membrane plane with the C and N termini on the lumenal side. The closeness of the C and N termini has been predicted earlier by cross-linking studies (*13*−*15*) and by analysis of the W241 emission properties (*16*). A structurally important element of the MSP is the conserved disulfide bridge between C28 and C51 in the spinach sequence, corresponding to the C19 and C44 residues in *Thermosynechococcus elongatus* (*17*, *18*).

The MSP is a protein of elongated shape with two major domains (*19*). Domain I is a cylinder composed of eight antiparallel $\beta$ strands, and its central part is occupied by hydrophobic amino acid residues. Domain II is an extended head, inserted between $\beta$ strands, and it mainly consists of

† This work was supported by grants from VR, The Swedish Foundation for International Cooperation in Research and Higher Education (STINT), and the KEMPE Foundation.

* To whom correspondence should be addressed. Telephone: +46-90-7865694. Fax: +46-90-7866676. E-mail: goran.samuelsson@plantphys.umu.se.

‡ Umeå University.

§ Russian Academy of Sciences.

|| New York University.

⊥ Linköping University.

[1] Abbreviations: ANS, 8-anilinonaphthalene-1-sulfonate; CD, circular dichroism; Chl, chlorophyll; DCBQ, 2,6-dichloro-*p*-benzoquinone; DTT, 1,4-dithiothreitol; EDTA, ethylenediamine bis($\beta$-aminoethyl ether)-*N*,*N*,*N*′,*N*′-tetraacetic acid; FTIR, Fourier transform infrared spectroscopy; HEPES, 4-(2-hydroxyethyl)-1-piperazineethanesulfonic acid; MES, 4-(*N*-morpholino)ethanesulfonic acid; MSP, manganese-stabilizing protein; PS II, photosystem II; SDS, sodium dodecyl sulphate; Tris, 2-amino-2-(hydroxymethyl)-1,3-propanediol; Trp, tryptophan; Tyr, tyrosine; WOC, water-oxidizing complex.

10.1021/bi0512750 CCC: $30.25 
Published on Web 10/27/2005

random coils and turns together with a distinct α helix. The apparent contradiction between extraordinary stability and flexibility of the MSP can be explained by the existence of one rigid "solid" part of MSP (domain I) and one flexible "liquid" part (domain II). The β barrel (domain I) is a very stable structure that is unlikely to differ whether the protein is free in solution or associated with PS II. In contrast, the hydrophilic loops (domain II) are stabilized by the interaction with other PS II proteins and are more flexible in the absence of those interactions, i.e., when the protein is not associated with PS II. A recent NMR study on overexpressed isolated MSP from cyanobacteria (*20*) also confirms that the MSP consists of two well-defined parts. Up to 40% of the protein, probably corresponding to domain II, has a high degree of flexibility on the pico- to nanoseconds time scale as was shown by NOE NMR data (*20*). In the same study, the authors pointed out that it is remarkably stable being exposed to different temperatures and pH values. Under illumination, the lumen becomes acidic (*21*). When the light intensity increases, the rates of electron transfer and proton release by PS II become greater, resulting in a substantial acidification of the thylakoid lumen that may damage the WOC and lead to subsequent release of manganese (*22*). Although it has been speculated that the β barrel of the PsbO protein provides a proton/water channel to the oxygen-evolving complex (OEC) (*23*), De Las Rivas and Barber (*19*) suggested recently that this is unlikely because the β barrel of PsbO is essentially solid with a hydrophobic inside. However, the authors proposed that a proton/water channel may be present outside the β barrel starting at D1−D61 and then proceeding along a hydrophilic pathway on the MSP. It may consist of the D158, D222, D223, D224, H228, and E229 residues facing into the lumen. Proton-dependent structural properties of the MSP were analyzed with respect to a decreasing lumenal pH upon illumination (*24*, *25*). Acid−base titration of the MSP demonstrated a characteristic hysteresis effect that is unique to the MSP and is accompanied by an increased accessibility to the hydrophobic core of the protein at lower pH. The near-UV circular dichroism (CD) of the MSP is altered at a lower pH, while the secondary structure remains virtually unchanged. Hence, the MSP changes its tertiary structure upon acidification of the aqueous environment but not its secondary structure. The existence of distinct and stable, proton-dependent conformational states (*24*, *26*) also reflects high flexibility of this protein with a putative functional relevance for photosynthetic water oxidation.

Metal ions affect the structure of MSP *in vitro*. Calcium and lanthanides induce a relative decrease of the unordered structure and β sheet and a substantial increase of the α helix, as was shown by FTIR spectroscopy (*27*). In contrast, in a recent study, the same approach demonstrated that the β structure is replaced by random coil (48 versus 38% of the β structure), while the α structure is not affected when $Ca^{2+}$ is added (*28*). No significant changes of the secondary structure in the presence of $Ca^{2+}$ ions were found by Kruk et al. (*29*), although CD spectra were affected by the presence of $Ca^{2+}$ or lanthanides. In the same study, a red shift of the tryptophan emission maximum was found, indicating calcium-induced unfolding of the MSP. In contrast, no changes of the cyanobacterial MSP secondary structure were observed by FTIR or CD in the presence of $Ca^{2+}$ ions, which according to Loll et al. (*30*) may reflect a difference between bacterial and higher plant MSP.

The functional implications of $Ca^{2+}$-induced structural changes of the MSP remain unclear. Heredia and De Las Rivas (*28*) proposed that $Ca^{2+}$-induced structural changes of the MSP may facilitate its binding to PS II. Kruk et al. (*29*) proposed that $Ca^{2+}$ bound to the MSP is different from the $Ca^{2+}$ of the $Mn_4CaO_4$ Cuban cluster of the oxygen-evolving center. The $Ca^{2+}$ bound to MSP would then not be directly involved in the photosynthetic oxygen evolution, although it may indirectly affect this process by influencing the conformation of the MSP.

Sequence analysis shows that the E93−E104 region of MSP from spinach is homologous to the $Ca^{2+}$-binding motif of "E-F hand" proteins (*31*), although the helix−loop−helix folding typical of "E-F hand" proteins is missing in the MSP tertiary structure (*12*). In addition, Heredia and De Las Rivas (*28*) recently found a similarity to the PRPSITE ps00330 hemolysin-type Ca-binding motif (D-x-[LI]-x(4)-G-x-D-x-[LI]-x-G-G-x(3)-D) sequence starting at D97 of the spinach MSP. Hemolysin-type calcium binding occurs in parallel β-roll structures that may have similarities to the MSP tertiary structure.

In this study, we present evidence for a model in which the MSP undergoes a pH-dependent conformational change that in turn influences its capacity to bind calcium and manganese ions.

## MATERIALS AND METHODS

*Isolation and Purification of the MSP*. PS II membrane fragments were prepared from spinach or pea leaves according to the procedure of Berthold et al. (*32*) with some modifications. The MSP was isolated from PS II membranes by salt-washing in two steps: first with 50 mM MES-NaOH (pH 6.0), 400 mM sucrose, and 1.5 M NaCl to remove 18- and 24-kDa proteins (NaCl-washed BBYs), followed by washing with 20 mM Tris-HCl (pH 9.0) and 1.5 M KCl including a proteinase inhibitor cocktail (Complete, Roche). After centrifugation at 40000*g* for 20 min, the supernatant was concentrated by ultrafiltration in an Amicon ultracentrifugal filter device (10 MWCO membranes) resulting in approximately 70% of recovery after ultrafiltration. The concentrated protein was dialyzed overnight against 20 mM MES-NaOH buffer (pH 6.5) containing 30 mM NaCl and further purified by chromatography on a Mono-Q column (Amersham, Biosciences). The MSP purification was conducted rapidly at +5 °C to minimize protein degradation. Insoluble material was removed from the sample by centrifugation (30000*g*, 15 min). The protein purity was checked on SDS/urea/PAGE using a mini-gel system (Bio-Rad Laboratory) combined with Coomassie staining (*33*, *34*). The electrophoresis was run with 20 μg of protein loaded per lane, which corresponds to approximately a 10-fold excess to detect impurities. The protein concentration was spectrophotometrically determined at a wavelength of 276 nm using the extinction coefficient of 16 $mM^{-1}$ $cm^{-1}$ as described by Eaton-Rye and Murata (*35*) and by the staining procedure developed by PIERCE (BCA protein assay).

The unfolded state of the MSP for control CD measurements was achieved by reduction of the only S−S bridge in a 1000-fold (mol/mol) excess of DTT. The apo form of the

protein was obtained by a two-step dialysis procedure, first against a buffer containing 20 mM MES (pH 6.5), 50 mM NaCl, and 5 mM EDTA and, second, against the same buffer without EDTA. Calcium and manganese were determined using a Perkin−Elmer 4100 ZL atomic absorption spectrometer with Zeemen background correction. Samples were diluted in 1% acetic acid prior to analysis.

*Spectroscopic Measurements.* Steady-state fluorescence experiments were conducted using a FluoroMax spectrofluorimeter with DM 3000F software (SPEX Industries, Inc.) and a custom-made spectrofluorimeter with registration from the front surface of the cell with some modifications (*36*). After correction for instrument spectral sensitivity, the intensities were proportional to the number of photons emitted in each wavelength interval. The bandwidth for both excitation and emission light did not exceed 2 nm. The protein concentration in fluorescence experiments was 1−3 $\mu$M. In measurements of intrinsic protein fluorescence, the excitation wavelength was 280.4 nm and emission spectra were recorded from 290 to 400 nm for each temperature. The area under the spectrum was normalized to a maximum value of 1.0 and plotted against the temperature in Figure 1. The fraction transition curves were calculated for tryptophan emission at the single band of wavelengths between 346 and 350 nm. The cuvette was maintained at a given temperature using a circulating water bath (Fisher Scientific). For 8-anilino-1-naphthalenesulfonate (ANS) fluorescence experiments, ANS was added to the buffer to a final concentration of 0.2 mM. The excitation and emission wavelengths used were 395 and 487 nm, respectively. Absorption spectra of protein samples were recorded on a MPS-2000 spectrophotometer (Shimadzu, Japan). CD spectra in the UV region were monitored with a Jasco J-800 spectropolarimeter at the optical path length of 1 mm. Calibration was carried out using a freshly prepared solution of D-camphor-10-sulfonate. The protein concentration was 30 $\mu$M. Prior to the spectroscopic measurements, the protein was desalted by dialyzing against 10 mM phosphate buffer (pH 7.2) and 10 mM NaCl and concentrated in an Amicon ultracentrifugal filter device (10 MWCO membranes).

The temperature gradient was performed stepwise, allowing the samples to equilibrate at each temperature for at least 5 min. The temperature was monitored directly inside the cell with a copper−constantan thermocouple.

*KOH Titration.* After the pH was adjusted to the desired value, the concentrated and desalted protein was added to a 2 $\mu$M final concentration. The KOH titration was made by addition of small aliquots (1−3 $\mu$L) of 20 mM KOH. When the deprotonation equilibrium was reached (depending upon pH, the time required varied from a few seconds to minutes), emission spectra of the samples were immediately recorded. Changes in pH were measured directly in the cuvette using a pH electrode connected to a MP230 pH-meter (Mettler TOLEDO).

*Analysis of Metal-Binding Isotherms.* Changes observed in ANS fluorescence upon addition of $Ca^{2+}$ or $Mn^{2+}$, $Q_{exp}$, were assumed (*37*) to be proportional to the degree of metal binding. The experimentally observed ANS emission, $Q_{exp}$, is described by

$$Q_{exp} = Q_0 + Q_1\overline{x_1} + Q_2\overline{x_2} \quad (1)$$

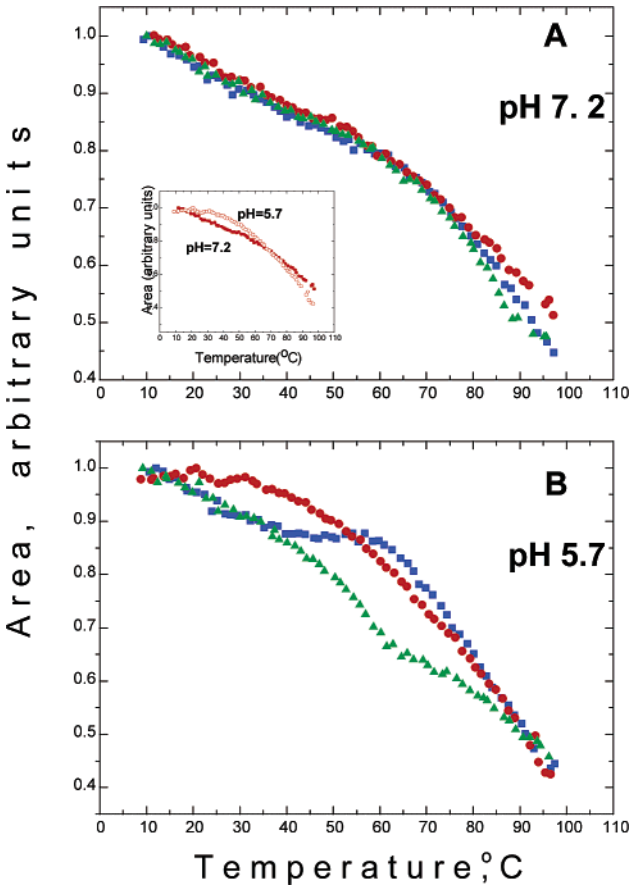


FIGURE 1: Temperature dependence of intrinsic fluorescence of isolated MSP at pH 7.2 (A) and 5.7 (B). No addition, red circles; in the presence of 2 mM $CaCl_2$, blue squares; and in the presence of 2 mM $MnCl_2$, green triangles. For a more clear comparison, the inset shows the temperature dependence of intrinsic fluorescence of MSP without additions at pH 7.2 and 5.7 also shown in A and B. Protein samples (0.3 mg/mL) were dissolved in 10 mM HEPES buffer (pH 7.2) or 10 mM MES buffer (pH 5.7). The temperature was increased stepwise, allowing the samples to equilibrate at each temperature for at least 5 min. The temperature was monitored inside the cell with a copper−constantan thermocouple. Fluorescence was excited at 280.4 and measured in the range between 290 and 400 nm. All spectra were corrected for the instrument spectral sensitivity. The standard deviation of three independent experiments was in average 8.4%.

where $Q_0$ is the ANS emission for apoprotein and $Q_1$ and $Q_2$ are the maximal changes in the spectroscopic probe induced by binding events.

The degree of binding was expressed as binding at two independent binding sites

$$\overline{x} = \overline{x_1} + \overline{x_2} = \frac{K_1[Me^{2+}]}{1 + K_1[Me^{2+}]} + \frac{K_2[Me^{2+}]}{1 + K_2[Me^{2+}]} \quad (2)$$

where $[Me^{2+}]$ is the total concentration of $Me^{2+}$ ($Ca^{2+}$ or $Mn^{2+}$ in our case), $\langle ob\rangle x_1\langle obx\rangle$ and $\langle ob\rangle x_2\langle obx\rangle$ are the degrees of binding, and $K_1$ and $K_2$ are the apparent binding constants for the first and second binding sites, respectively (*37*).

*Light versus Dark Extraction of MSP*. The removal of the MSP from PS II membranes was done by two different approaches: heat and pH treatments. Heat treatment of BBY particles lacking the 18- and 24-kDa extrinsic proteins (NaCl-washed BBY particles) was carried out at 0.5 mg of Chl

$mL^{-1}$ for 7 min at 45 °C in a water bath. The medium contained 5 mM MES buffer (pH 6.5) and 200 mM sucrose, and the procedure was conducted either under illumination or in darkness. The pH treatment was done at 0.075 mg of Chl $mL^{-1}$ for 30 min at 10 °C in a water bath. This procedure was conducted in a medium containing 20 mM buffer (MES for pH 5.7 and HEPES for pH 7.2) and 0.1 M sucrose either under illumination or in darkness. Illumination of the sample during both treatments was done as follows: the suspension of NaCl-washed BBY particles was placed in a glass cuvette in a water bath and illuminated with white light at 120 $\mu$mol $m^{-2}$ $s^{-1}$ in the presence of 0.1 mM DCBQ and 0.5 mM FeCN. The dark sample was incubated under the same conditions without illumination. After incubation at desired conditions, samples were centrifuged and the pellet and supernatant were analyzed separately on SDS/urea/PAGE and Western blot. Immunoblotting was performed as described in the protocol supplied by Bio-Rad Laboratories. Horseradish peroxidase-labeled secondary antibodies and enhanced chemiluminescence (ECL, Amersham Biosciences) were used to detect the antibody−antigen conjugate. The protein amount in gels and blots were estimated by the Gel-Pro Analyzer (Media Cybernetics, Inc.) program after calibration.

## RESULTS

*Intrinsic Fluorescence of the MSP*. It was shown earlier (*16*, *38*, *39*) that the MSP is characterized by rare fluorescent properties. Fluorescence by the only tryptophan residue (W241), usually dominating in protein emission, is considerably quenched in contrast to tyrosine fluorescence. Therefore, the emission spectrum of native MSP has a maximum at 308 nm (tyrosine), while the fluorescence of W241 (with a maximum at 330 nm) is revealed only as a shoulder (*16*). Upon denaturation of the MSP, the tryptophan fluorescence becomes dominant because of an increased distance between W241 and the proposed quenching S−S bridge (*16*).

Figure 1A (red circles) shows that at pH 7.2 the fluorescence of the MSP (see the Materials and Methods) is characterized by a monotonic increase in quenching with an increasing temperature from 10 to 95 °C. There are virtually no changes in this melting curve if $MnCl_2$ (2 mM) or $CaCl_2$ (2 mM) are added before the measurements (green triangles and blue squares, respectively), except perhaps at the very highest temperatures. When the protein in the absence of $Ca^{2+}$ and $Mn^{2+}$ is transferred to a medium at pH 5.7, its melting curve is altered in the region 20−65 °C, compared to at pH 7.2, while at the highest temperatures, the two melting curves differs slightly but in an opposite direction (compare the solid and open red circles in the inset of Figure 1A). Notably, at pH 5.7, the thermal transition becomes sensitive to the presence of 2 mM $MnCl_2$ and 2 mM $CaCl_2$ (Figure 1B, green triangles and blue squares, respectively). Upon the addition of $Ca^{2+}$ or $Mn^{2+}$ at pH 5.7, the melting curve becomes similar to the curve obtained for the protein at pH 7.2 in the region 20−45 °C (compare parts A and B of Figure 1). In the temperature interval 45−85 °C, the effects of added $Ca^{2+}$ and $Mn^{2+}$ are quite different: (1) $Ca^{2+}$ brings the curve back to the melting observed for the protein at pH 5.7 without additions, while (2) $Mn^{2+}$ shifts the melting curve to lower temperatures. The effect of addition of 2 mM $MgCl_2$ on the melting curve was very similar to that observed for 2 mM $CaCl_2$ (data not shown).

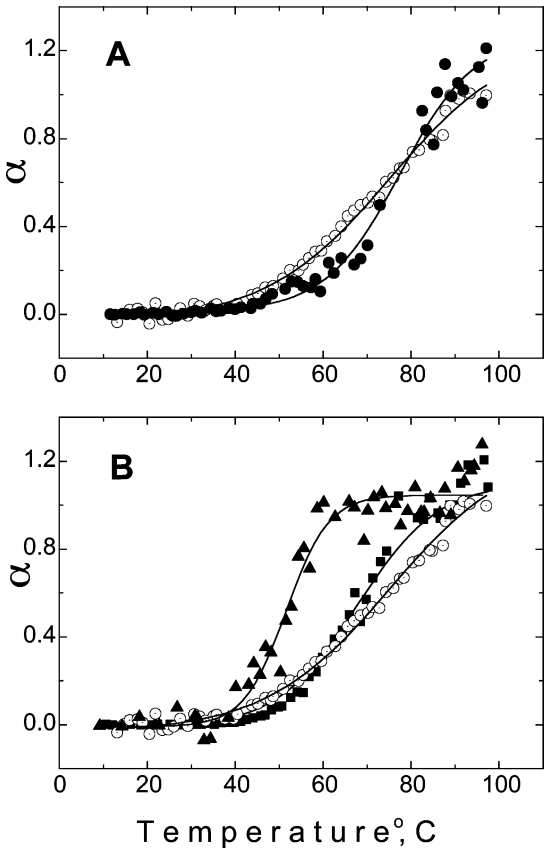


FIGURE 2: Normalized curves of fraction conversion $\alpha = \langle fr\rangle[P_0]\langle fd\rangle([P_1] + [P_2])\langle frx\rangle$ calculated from the fluorescence intensity data shown in Figure 1. (A) MSP with no addition at pH 5.7 (○) and 7.2 (●). (B) MSP at pH 5.7 without addition (○), loaded with 2 mM $MnCl_2$ (▲), and 2 mM $CaCl_2$ (■). The fraction of conversion was calculated from the plots of temperature dependence of emission intensity at a fixed wavelength as previously described (*40*).

It is important to note that in agreement with a previous report (*16*) the emission spectrum of the MSP differed from the random coil spectrum at 95 °C, indicating that the protein is not completely unfolded even at 95 °C.

To obtain a more detailed analysis of the melting curves shown in Figure 1, they were recomputed as fraction conversion curves using an approach described earlier (*40*). The results of this analysis are presented in Figure 2. At pH 7.2, the melting point ($T_m$) (corresponding to a 50% transition) of the protein is near 75 °C or higher (● in Figure 2A and Table 1). It is difficult to make a more precise determination of $T_m$ because the transition is not cooperative; it progresses over a broad range of temperatures and is not complete even at 95 °C. Similar $T_m$ values of 75−77 °C are observed at pH 7.2 in the presence of $Ca^{2+}$ and $Mn^{2+}$ (Table 1).

At pH 5.7, the fraction conversion curve of the MSP is even less cooperative than at pH 7.2 probably because of the mixing of several transition states: it takes place in a wide temperature range (more than 40 °C), with a $T_m$ value near 72 °C (Figure 2A, ○). The additions of $Ca^{2+}$ or $Mn^{2+}$ at pH 5.7 result in a considerable shift of the melting point to lower temperatures. In the presence of $Ca^{2+}$ and $Mn^{2+}$, the $T_m$ is 68 and 52 °C, respectively (Figure 2B, ■ and ▲). Besides, in the presence of metals, the transitions become more cooperative.

Table 1: Melting Points ($T_m$, °C) of Thermal Transitions of the MSP

| conditions/ transitions | low-temperature transition (°C) | high-temperature transition (°C) |
|---|---|---|
| pH 7.2, no additions | | 77[a] |
| pH 7.2, + $Ca^{2+}$ | | 75[a] |
| pH 7.2, + $Mn^{2+}$ | | 75[a] |
| pH 6.5, no additions | | 76 (*30*) |
| pH 6.0, + $Ca^{2+}$ | 56 (*28*) | |
| pH 5.7, no additions | | 72[b], 75[a], 76[c] |
| pH 5.7, + $Ca^{2+}$ | | 68[a], 70[b] |
| pH 5.7, + $Mn^{2+}$ | 52[a] | 68[b] |

[a] $T_m$ calculated from the thermal transition monitored by intrinsic fluorescence. [b] $T_m$ calculated from the thermal transition monitored by CD at 202 nm. [c] $T_m$ calculated from the thermal transition monitored by CD at 293 nm.

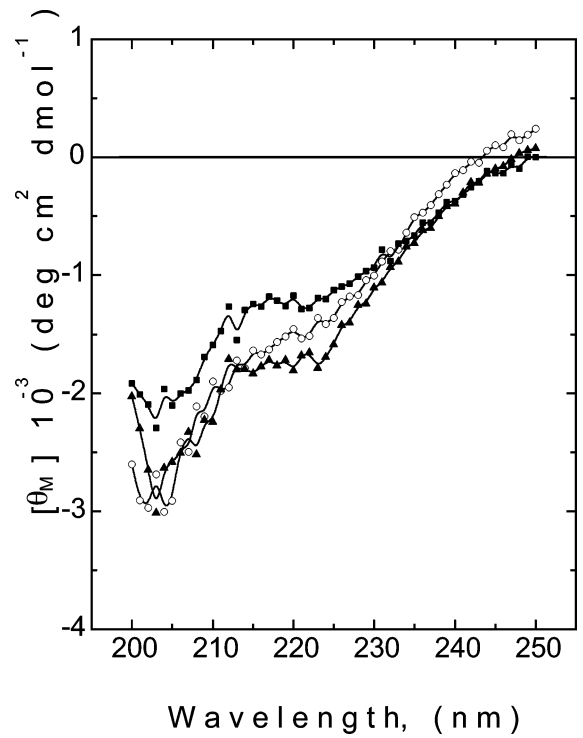


FIGURE 3: CD spectra of MSP in 10 mM phosphate buffer at pH 5.7 recorded at 95 °C. No addition (○), in the presence of 2 mM $CaCl_2$ (■), and in the presence of 2 mM $MnCl_2$ (▲). The spectra represent three independent experiments.

*CD Measurements.* The thermal unfolding of the MSP at pH 5.7 monitored by CD at 202 nm was analyzed using a model described earlier (*41*). The experimental results from three independent repetitions were fitted to this model, and the thermal unfolding of MSP was ascribed to a two-state transition. The midpoint of the thermal transition of the MSP is at 72 °C. The addition of $Ca^{2+}$ or $Mn^{2+}$ ions shifts this value lower to 70 and 68 °C, respectively (see Table 1).

In agreement with earlier studies (*30*, *42*), the far-UV CD spectrum of the MSP at 95 °C (Figure 3) differs from the random coil spectrum. The unfolded state of the MSP was achieved only by reduction of the S−S bridge but not by heating to 98 °C (data not shown). These results suggesting that the MSP is not completely unfolded at 95 °C.

The presence of $Mn^{2+}$ and $Ca^{2+}$ slightly changes the far-UV CD spectrum of the MSP at both 25 and at 95 °C, but it remains distinct from the random coil spectrum.

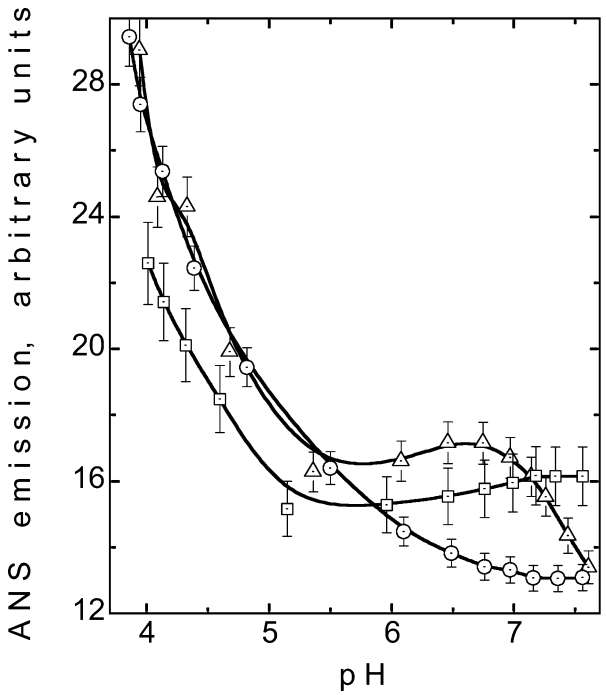


FIGURE 4: Fluorescence emission intensity of ANS in the presence of 1 $\mu$M MSP as a function of pH. No addition (○), in the presence of 2 mM $CaCl_2$ (□), and in the presence of 2 mM $MnCl_2$ (△). The excitation wavelength was 395 nm, and the fluorescence emission was measured at 485 nm at 25 °C. The change of pH in the range 4.0−7.5 was achieved by the addition of KOH to the protein solution. See the Materials and Methods for details of the assay conditions. Error bars represent three independent experiments.

*ANS Fluorescence Measurements.* It is well-established that fluorescence emitted by ANS can be used for monitoring structural changes of proteins. The fluorescence of free ANS in water solution in the absence of MSP is independent of pH in the range from 3.8 to 7.8 (data not shown and ref *43*). In agreement with previous work (*24*), we show that the addition of MSP at pH 3.8 leads to a 4.5-fold increase of the ANS fluorescence. Subsequent addition of KOH aliquots leads to a progressive decrease of the ANS emission (Figure 4, ○). This indicates that the hydrophobic core of MSP responds to pH changes by opening at acidic pH and closing at neutral pH. Without additions of $Ca^{2+}$ or $Mn^{2+}$ ions, the pH dependence of ANS fluorescence has a monotonic character (Figure 4, ○) reflecting the transition of the MSP from an open to closed form with the pH increase. Upon addition of $Ca^{2+}$ and $Mn^{2+}$ to the MSP in solution, the pH dependence of ANS fluorescence intensity is considerably altered (Figure 4, □ and △, respectively). In the presence of 2 mM $MnCl_2$, the fluorescence begins to increase again at about pH 5.5, it reaches a peak at pH 6.5, and drops off again to the low value (Figure 4, △) seen in the absence of metal additions at about pH 7.5 (Figure 4, ○). Also in the presence of 2 mM $CaCl_2$, there is an increase in fluorescence beginning at about the same pH as for $MnCl_2$, but unlike for $MnCl_2$, there is no peak or drop off in fluorescence intensity at the higher pH values (Figure 4, □).

Changes in the ANS fluorescence intensity measured at pH 5.7 upon the addition of $Ca^{2+}$ or $Mn^{2+}$ were analyzed according to eqs 1 and 2 to estimate the apparent metal-binding constants. A comparison of isotherms fitted to the experimental results is presented as Supporting Information. The calculations show that there are two binding sites for

each metal in the MSP molecule at pH 5.7 with different affinity; one $Ca^{2+}$ binding site has an apparent binding constant of $\approx 10^6$ $M^{-1}$, and one $Mn^{2+}$ binding site has an apparent binding constant of $\approx 10^4$ $M^{-1}$. A very low-affinity binding site with an apparent binding constant of $\approx 10^2$ $M^{-1}$ is the same for both $Ca^{2+}$ and $Mn^{2+}$, which means that binding at this site would occur only above physiological concentrations. Presumably, the apparent binding constant of $\approx 10^2$ $M^{-1}$ may reflect unspecific binding of $Ca^{2+}$ to the $Mn^{2+}$ binding site and $Mn^{2+}$ to the $Ca^{2+}$ binding site. Nevertheless, because $Ca^{2+}$ binding induced changes of the MSP melting curve that were different from those induced by $Mn^{2+}$ binding (compare green triangles and blue squares in Figure 1B), the presence of different binding sites for $Ca^{2+}$ and $Mn^{2+}$ is strongly suggested.

*Light and Dark Extraction of $Mn^{2+}$ and MSP from PS II.* The results described above for MSP in solution raise the question whether the low pH-induced conformational change followed by $Ca^{2+}$ and $Mn^{2+}$ binding by the MSP also occurs when MSP is bound to the PS II reaction centers? To compare the ability of the MSP to bind $Mn^{2+}$ in its light acidic and dark basic conformations, NaCl-washed BBY particles lacking the 18- and 24-kDa extrinsic proteins were exposed to darkness or light during extraction of MSP. The light intensity and illumination time were considerably smaller than those typically used in photoinhibition studies (120 versus 1000 mol $m^{-2}$ $s^{-1}$ and 7−30 versus 30−120 min). The low light intensity and the presence of exogenous electron acceptors in the reaction media mantain functionally active PS II reaction centers during illumination.

Figure 5 shows results obtained by light and dark extraction of the MSP by heat treatment of NaCl-washed PS II membrane fragments. The SDS−PAGE profile of the pellet after the heat treatment (Figure 5B) demonstrates that the 33-kDa band corresponding to the MSP is less prominent in the light-treated membranes compared to that of dark-treated membranes. The intensity of all other protein bands is similar in the samples from both treatments. These data were further confirmed by immunoblot analysis of the supernatant (Figure 5A). When heat treatment of NaCl-washed PS II membrane fragments was carried out in light, the amount of MSP found in the supernatant was greater than in the dark. It appears that, under illumination, the interaction of the MSP with PS II is weakened and that the heat extraction of the MSP is therefore more efficient. Figure 5C depicts the quantification of the MSP remaining bound in the pellet (left axis and left bars) after the heat solubilization of MSP shown in Figure 5B. The amount of remaining bound MSP is in good agreement with the amount of remaining manganese calculated per PS II reaction center (230 Chl) (Figure 5C, right axis and right bars). The amount of both MSP and manganese in the insoluble fraction is approximately 3 times smaller in samples extracted in the light than in the dark.

Figure 6 reports light and dark extraction at 10 °C of MSP and $Mn^{2+}$ at pH 5.7 and 7.2, the same pH values as were used in the *in vitro* study as discussed above. In agreement with the results of the heat solubilization of MSP, the amount of the MSP in the supernatant is greater in the light sample than in darkness at both pH 5.7 and 7.2. Preincubation of BBY particles in darkness at high pH prevents MSP to form the "open conformation" and also abolishes the effect of illumination (data not shown). Furthermore, in agreement

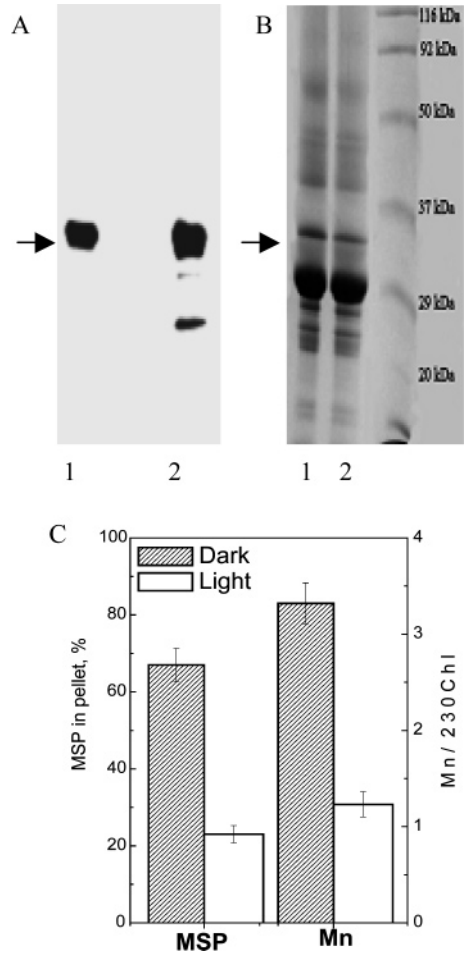


FIGURE 5: Extraction of MSP and manganese from NaCl-washed BBY particles by heat treatment. (A) Immunoblot analysis of the supernatant with antibodies raised against spinach MSP and (B) polypeptide profiles of the pellet after staining with Coomassie Blue. Lanes 1 and 2 are for extraction in the dark and light, respectively. (C) Amount of MSP and manganese remaining in PS II membrane fragments after the heat treatment. Light samples, open bars; and dark samples, hatched bars. Error bars represent three independent experiments. Equal amounts of samples on a Chl basis were used for SDS−PAGE. For more experimental details, see the Materials and Methods.

with the intrinsic and ANS fluorescence data (Figures 1, 2, and 4), we found only 0.1 $Mn^{2+}$/MSP at pH 7.2 after either light or dark extraction, whereas after light extraction, there were 1.24 $Mn^{2+}$/MSP at pH 5.7. Because of the very small amount of protein extracted in the dark at this pH, the estimate of the amount of $Mn^{2+}$ per protein is rather uncertain.

These data indicate that the conformation of MSP and its binding to PS II are different in light and darkness and that extraction of MSP under illumination correlates with the release of manganese and calcium (data not shown).

## DISCUSSION

The combined results from our spectroscopic studies clearly show that the interaction of both $Mn^{2+}$ and $Ca^{2+}$ with the isolated MSP is dependent upon pH within the physiological pH range. At pH 7.2, neither of the metal ions changes the melting curve of MSP, while at pH 5.7, it is significantly modified by both $Mn^{2+}$ and $Ca^{2+}$ (Figure 1). Instead of an expected decrease of metal binding upon

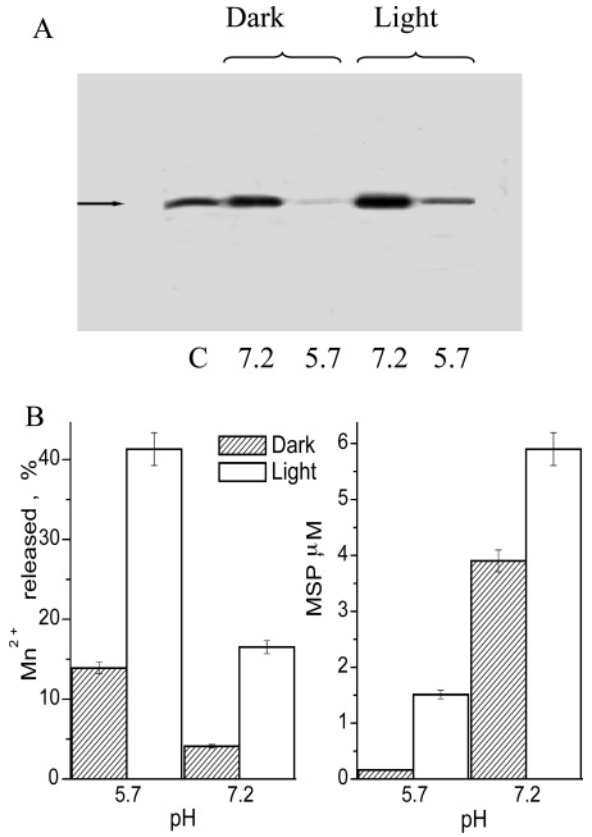


FIGURE 6: Light and dark extraction of MSP and manganese from NaCl-washed BBY particles at pH 5.7 and 7.2. (A) Immunoblots of the soluble fractions using antibodies raised against spinach MSP after extraction at the indicated pH values. The overexpressed spinach MSP with a known concentration was used as a control (lane C in A). (B) Amounts of manganese and MSP found in the supernatant after extraction. Light samples, open bars; and dark samples, hatched bars. Equal amounts of samples on a Chl basis during extraction were used for SDS−PAGE. For more experimental details, see the Materials and Methods.

lowering of pH because of the competition with $H^+$ for the negatively charged binding sites, as in α-lactalbumin (*44*), the MSP interaction with $Mn^{2+}$ and $Ca^{2+}$ is much stronger at pH 5.7 than at pH 7.2. This could be due to a rearrangement of the MSP at low pH, resulting in a greater accessibility of negatively charged groups involved in $Mn^{2+}$ and $Ca^{2+}$ binding. The ability to bind $Mn^{2+}$ and $Ca^{2+}$ coincides with the pH range where the acid−base hysteresis of the buffer capacity of the MSP occurs (*24*). This hysteresis effect is most likely dependent upon the existence of two different MSP conformations. One of these conformations is characterized by an unusually high p*K* of approximately 5.7 for an estimated 12 aspartate or glutamate residues (*24*, *25*). Therefore, the existence of two pH-dependent conformations of the MSP is likely to be responsible for the $Mn^{2+}$ and $Ca^{2+}$ effect on the protein melting curves.

The thermal unfolding of MSP from both cyanobacteria and higher plants has been studied intensively over the years (*28*−*30*, *42*, *45*). A sigmoidal unfolding pattern in a broad temperature range with a melting point of 61−65 °C was observed by CD measurements for the spinach MSP (*42*). Upon cooling, the heat-treated protein returns to a near native state and is capable of rebinding and reactivating the oxygen evolution activity of PS II (*42*). Differential scanning calorimetry curves of the spinach MSP exhibit an endothermic peak with a $T_m$ of 63 °C and a broad transition in the range of 80−100 °C. The protein is not irreversibly denaturated even at 125 °C. Addition of $Ca^{2+}$ or lanthanides shifts the $T_m$ toward lower temperatures (*29*). A melting point of 56 °C and a sigmoidal curve with a second phase above 60 °C was determined by FTIR (*28*) for spinach MSP in the presence of $Ca^{2+}$. Moreover, the amount of β structure at 60 °C is the same as at 20 °C. Heredia and De Las Rivas (*28*) suggested that MSP reaches an intermediate state between 60 and 70 °C and that one part of the protein can undergo a quick and energetically favorable unfolding, while another part of it forms a hydrophobic core that withstands denaturation (*28*). Sonoyama and co-workers (*45*) showed that thermal unfolding of the cyanobacterial MSP is a reversible process and is due to unfolding of the β structure rather than the α structure. A temperature-dependent transition with a $T_m$ of 76 °C, as noted by the increase of the negative CD signal at 222 nm, of cyanobacterial MSP was reported recently (*30*). It is not clear why MSP from *Thermoseneccococus elongatus* has greater thermostability than spinach MSP because both have the same proportion of disordered structure and the same content of proline residues (*20*). The discrepancy between $T_m$ values obtained in different experiments for higher plant MSP, as well as between higher plant and cyanobacterial MSP, may be due to different pH values used in the experiments and/or the presence of different amounts of metal ions depending upon the isolation method.

The $T_m$ value of MSP without additions of $Mn^{2+}$ and $Ca^{2+}$ at pH 5.7 obtained in our study from the CD signal in the near UV region at 293 nm coincides with the value obtained from the intrinsic protein fluorescence, 76 and 75 °C, respectively (Table 1). Both approaches monitor the microenvironment of the aromatic amino acid residues, although the dominant part is from W241. The fraction conversion curves were calculated specifically for tryptophan emission at the single band of wavelengths between 346 and 350 nm (see the Materials and Methods); therefore, these curves reflect temperature-induced changes of the W241 microenvironment in the lumenal part of the β barrel (domain I). In contrast, CD in the far-UV region, where peptide bonds absorb the light, reflects the increase of the random coil fraction upon heating. The $T_m$ value calculated from the CD signal at 202 nm is also in agreement with $T_m$ calculated from CD at 293 nm and fluorescence, 72 versus 76 and 75 °C, respectively (Table 1). This indicates changes of both the protein secondary structure and the W241 environment at this temperature.

Metal binding usually leads to stabilization of the protein structure (*46*) and shifts the melting curves to a higher temperature range. As follows from the analysis of the MSP melting curves (Figure 2), $Ca^{2+}$ and especially $Mn^{2+}$ lower the melting point of the MSP at pH 5.7.

The addition of $Ca^{2+}$ leads to shifts of the $T_m$ values toward lower temperatures by 2 °C from far-UV CD and of 7 °C from fluorescence measurements. In the presence of $Ca^{2+}$, the $T_m$ values determined by far-UV CD and fluorescence are very similar (within 2 °C). Therefore, the thermal transition of the MSP in the presence of $Ca^{2+}$ also appears to involve both the secondary structure and the W241 environment.

A different pattern was observed when $Mn^{2+}$ was added to the MSP solution, because then the protein exhibits two temperature-induced transitions. One transition at 68 °C is observed by far-UV CD and involves changes of the protein secondary structure. Another transition at 52 °C is characterized by high cooperativity and involves changes of the W241 microenvironment observed by intrinsic protein fluorescence. In the presence of $Mn^{2+}$, the shift of the $T_m$ value as measured as fluorescence, is more than 20 °C compared to MSP without added $Mn^{2+}$. The simultaneous lowering of $T_m$ and the increase of the transition cooperativity may reflect that $Mn^{2+}$ induces the formation of a local but well-structured domain within the protein, probably in the lumenal part of the $\beta$ barrel.

Our results demonstrate the presence of two independent metal-binding sites in the MSP molecule with different affinity for $Ca^{2+}$ and $Mn^{2+}$. These two binding sites induce different changes of the MSP conformation at pH 5.7 (Figures 1, 2, and 4). To observe maximal metal-induced changes in the MSP structure, we used identical and saturating concentrations of $Ca^{2+}$ or $Mn^{2+}$ (2 mM). Under these conditions, $Mn^{2+}$ can probably bind to both metal-binding sites. It may bind unspecifically to the $Ca^{2+}$ binding site (because of the $Mn^{2+}$ concentration being about 1000 times in excess of the apparent binding constant) and specifically to the $Mn^{2+}$ binding site. Therefore, we attribute the low-temperature transition to specific binding of $Mn^{2+}$ to the $Mn^{2+}$ binding site and the high-temperature transition to unspecific binding of $Mn^{2+}$ to the $Ca^{2+}$ binding site. At the same time, both $Mn^{2+}$ and $Ca^{2+}$ shift the $T_m$ value to lower temperatures. This is consistent with the destabilization effect of $Ca^{2+}$ binding to MSP in agreement with previous reports (*28*, *29*).

The effect of both $Mn^{2+}$ and $Ca^{2+}$ is less in the CD measurements than in the measurements of the intrinsic MSP fluorescence (Table 1). The fluorescence effects are related to changes in the lumenal side of the $\beta$ barrel because tryptophan W241 is located inside the $\beta$ barrel at the lumenal terminus (Figure 7). Our calculations of the number of W241 neighbors of the modeled spinach MSP structure suggests that there are 14 amino acid residues located within a 4 Å distance from W241. This corresponds to 5.7% of the entire MSP sequence. The fact that the addition of neither $Ca^{2+}$ nor $Mn^{2+}$ did much affect on the secondary structure composition calculated from far-UV CD spectra although the spectra themselves differed (ref *29* and our data) indicates that the number of residues involved in the metal-induced changes are too small to estimate changes in the secondary structure. In contrast, FTIR experiments have shown a 7−10% decrease of the $\beta$ structure in the presence of $Ca^{2+}$ (*28*). The common notion is thought that CD provides more accurate estimations of the α structure, whereas FTIR is more sensitive to $\beta$ sheets (*47*). Another explanation could be the high protein concentration required for FTIR measurements, which can cause aggregation of the protein. Because signs of aggregation were observed in these experiments at temperatures above 70 °C and because $Ca^{2+}$ induced changes in the MSP $\beta$ structure at room temperature, we believe that this is due to a macromolecular-crowding effect at high protein concentrations (*48*, *49*), rather than to aggregation.

Our ANS fluorescence measurements suggest that the accessibility of the hydrophobic regions of the MSP increases considerably upon the transition from the alkaline conformation to the acidic conformation. This supports our idea of the formation at low pH of the open-state protein conformation with more exposed hydrophobic residues. The monotonic change from the state with closed hydrophobic patches at neutral pH to more exposed hydrophobic residues at lower pH is further tuned by the addition of $Mn^{2+}$ and $Ca^{2+}$ (Figure 4). The $Mn^{2+}$-induced increase of ANS fluorescence in the pH region between 6.5 and 5.5 may reflect an opening of the hydrophobic core upon $Mn^{2+}$ binding. The same behavior was reported for $Ca^{2+}$-sensor proteins involved in transduction of intracellular $Ca^{2+}$ signals. These proteins expose a hydrophobic area on the surface in response to $Ca^{2+}$ binding (*50*), in contrast to $Ca^{2+}$-buffering proteins that remain "closed" after binding.

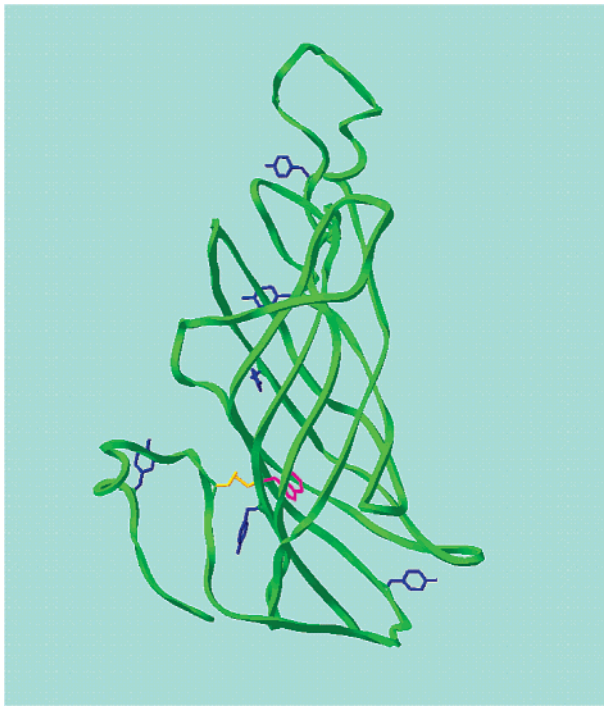

FIGURE 7: Location of C, Y, and W residues in the manganese stabilizing protein from *Spinacea oleacia*. The structural model was build using the Swiss-Model program (*54*). PsbO 3D structures were obtained from the PDB database. Tyrosine residues are given in blue; the S−S bridge is given in orange; and the tryptophan residue is given in magenta. This figure was generated with Deep View/Swiss-Pdb Viewer 3.7 (SP5).

$Mn^{2+}$ does not change the fluorescence of ANS in the presence of MSP at pH above 7.2. This is consistent with the notion of a weak interaction of $Mn^{2+}$ with MSP at neutral pH. However, a $Ca^{2+}$-induced change is observed in contrast to the response to $Mn^{2+}$ at this pH. In contrast, measurements of the thermal transitions of the intrinsic fluorescence suggest that $Ca^{2+}$ does not interact efficiently with MSP at this pH. This discrepancy may at least in part be due to the difference in the influence of $Ca^{2+}$ and $Mn^{2+}$ on the MSP conformational state and/or on the probes used in those experiments. ANS fluorescence reflects changes in the accessibility of the hydrophobic core inside the $\beta$ barrel, while the intrinsic fluorescence reflects environmental changes around tyrosines and W241 located mainly on the lumenal side of the $\beta$ barrel (Figure 7).

The study of MSP *in vitro* reported here leads to the conclusion that the interaction of the MSP with $Ca^{2+}$ and

$Mn^{2+}$ is greater at pH 5.7 than at pH 7.2. This acidic pH occurs *in vivo* in the lumen under illumination (*21*); therefore, in the light, the MSP appears to be "open" and the binding sites are accessible to $Ca^{2+}$ and $Mn^{2+}$. The lack of effects of $Ca^{2+}$ and $Mn^{2+}$ on the isolated MSP at pH 7.2 suggests that in darkness *in vivo* the MSP, when it is associated with PS II and the pH is typically about 7.5, interacts only weakly with $Ca^{2+}$ and $Mn^{2+}$ because the MSP is more "closed" and the binding sites are inaccessible to $Ca^{2+}$ and $Mn^{2+}$. To test if the acid conformation of MSP also exists when it is bound to the PS II reaction centers and can bind $Mn^{2+}$ and/or $Ca^{2+}$, we studied the extraction of manganese and MSP from PS II in light and darkness. The results demonstrate that illumination weakened the interaction of the MSP with PS II (Figures 5 and 6) and that there is a positive correlation between the amount of extracted MSP and the release of $Mn^{2+}$ and $Ca^{2+}$. Moreover, MSP must be in its "open conformation" to cause a difference in extractability of MSP and manganese between light- and dark-exposed PS II particles. Our results suggest that a local pH effect caused by protons released from PS II may be more important for MSP conformation than that of the bulk pH (see Figure 6). However, we cannot rule out the possibility that the MSP docking site is affected by illumination. More experiments are required to resolve this issue. We hypothesize that protonation of amino acid residues in MSP located close to the Mn cluster by protons from water splitting is responsible for the conformational changes of MSP rather than those located on the surface of the protein. Preliminary evidence suggests that those amino acid residues responsible for interactions between MSP and the membrane are the sensor for protons *in vivo* and cause the light-induced conformational changes of MSP. In solution, these residues will be exposed and can hence sense free protons in solution. However, when attached to the lumen side of the thylakoid membrane, these residues will be concealed from bulk protons. Therefore, bulk pH will not give the same effect on the MSP structure when it is associated to the membrane as free MSP in solution.

This is a first attempt to link a study of the MSP *in vitro* to the function of this protein *in vivo* at low protein concentrations. FTIR that also has been used for this purpose (*51*, *52*) requires much higher protein concentrations. Our results allow us to propose that under nonphotoinhibiting light the interaction of MSP with PS II is weaker compared to in the dark, probably because of light-induced conformational changes in the MSP.

Several functional implications of the pH (light) dependent conformational change and $Ca^{2+}$ and $Mn^{2+}$ binding of MSP for PS II activity may be suggested.

(a) The high flexibility of MSP and its open conformation at lower pH may be important for both providing and regulating accessibility of water to the WOC and removal of protons from the WOC.

(b) The MSP binds manganese and calcium released upon photoinhibition that are required for repair of the WOC after photoinhibition.

(c) The MSP may be involved in a reversible dissociation reaction of the $Mn_4Ca$ complex of the WOC under physiological conditions.

Earlier it was suggested that up to 12 negatively charged amino acid residues with an unusually high p*K* may be

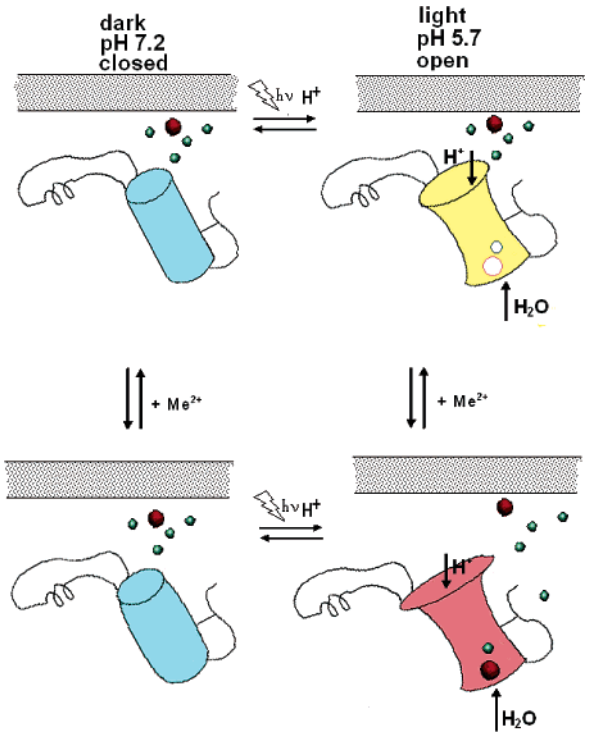


FIGURE 8: Model describing the $H^+$- and metal-induced conformational changes of the MSP. Protonation of the MSP is proposed to change its conformation so that it becomes able to bind $Mn^{2+}$ and/or $Ca^{2+}$. Manganese atoms are given in green, and calcium atoms are given in red. Binding of $Mn^{2+}$ and/or $Ca^{2+}$ causes a second conformational change facilitating the movement of water to and protons from WOC.

important for regulation of proton and water exchange within the WOC (*24*). Using mass spectroscopic measurements, it was recently shown by Hiller and Wydrzynski (*53*) that the rate of water exchange with the WOC is slowed by removal of the MSP.

Our proposed model of pH-dependent $Ca^{2+}$ and $Mn^{2+}$ binding to the MSP is summarized in Figure 8. At pH 7.2, typical of darkness, MSP interacts only weakly with $Ca^{2+}$ and $Mn^{2+}$. Light-induced protonation of the MSP (pH 5.7) leads to a protein conformation with more exposed hydrophobic residues. It is assumed that protons released during water oxidation bind to the MSP and change it from a closed to an open conformation. In the light-induced open conformation, the interaction of the MSP with $Ca^{2+}$ and $Mn^{2+}$ becomes stronger. There are two metal-binding sites in the MSP molecule with different affinities for manganese and calcium (shown in green and red in Figure 8). The binding of $Ca^{2+}$ and $Mn^{2+}$, in turn, is accompanied by a second conformational change. All conformational changes represented in this model are reversible. Thus, the results reported in this paper suggest that the transition from the closed state at neutral pH to the open state at low pH is relevant for regulation of the binding of $Mn^{2+}$ and $Ca^{2+}$ and for the regulation of the function of the WOC.

## ACKNOWLEDGMENT

We are grateful to Professor B. Martin for fruitful discussions and critical comments on the manuscript.

## SUPPORTING INFORMATION AVAILABLE

Changes in the ANS fluorescence intensity as a function of the concentration of $Ca^{2+}$ and $Mn^{2+}$ in the presence of MSP measured at pH 5.7. Symbols, experimental results; lines, the fit of experimental data to eq 2 as described in the Materials and Methods. This material is available free of charge via the Internet at http://pubs.acs.org.

## REFERENCES


1. ) Debus, R. (2001) Amino acid residues that modulate the properties of tyrosine Y−Z and the manganese cluster in the water oxidizing complex of photosystem II, *Biochim. Biophys. Acta 1503*, 164−186.
2. Renger, G. (2001) Photosynthetic water oxidation to molecular oxygen: Apparatus and mechanism, *Biochim. Biophtys. Acta 1503*, 210−228.
3. Bricker, T. (1992) Oxygen evolution in the absence of the 33-kDa manganese stabilizing protein, *Biochemistry 31*, 4623−4628.
4. Seidler, A. (1996) The extrinsic polypeptides of photosystem II, *Biochim. Biophys. Acta 1277*, 35−60.
5. De Las Rivas, J., Balsera, M., and Barber, J. (2004) Evolution of oxygenic photosynthesis: Genome-wide analysis of the OEC extrinsic proteins, *Trends Plant Sci. 9*, 18−25.
6. Miyao, M., and Murata, N. (1984) Role of the 33-kDa polypeptide in preserving Mn in the photosynthetic oxygen-evolution system and its replacement by chloride ions, *FEBS Lett. 170*, 350−354.
7. Ono, T., and Inoue, Y. (1984) Reconstitution of photosynthetic oxygen evolving activity by rebinding of 33 kDa protein to $CaCl_2$-extracted PS II particles, *FEBS Lett. 166*, 381−384.
8. Vass, I., Ono, T., and Inoue, Y. (1987) Stability and oscillation properties of thermoluminescent charge pairs in the $O_2$-evolving system depleted of $Cl^-$ or the 33 kDa extrinsic protein, *Biochim. Biophys. Acta 892*, 224−235.
9. Burnap, R. L., and Sherman, L. A. (1991) Deletion mutagenesis in *Synechocystis* sp. PCC6803 indicates that the Mn-stabilizing protein of photosystem II is not essential for $O_2$ evolution, *Biochemistry 30*, 440−446.
10. Hiramatsu, H., Mizobuchi, A., Mori, H., and Yamamoto, Y. (1991) Relationship between the stability of antenna Chl α-binding proteins CP43/47 and the accumulation of the extrinsic 30-kDa protein in PS-II in *Euglena*. *Plant Cell Physiol. 32*, 881−889.
11. Spetea, C., Hundal, T., Lundin, B., Heddad, M., Adamska, I., and Andersson, B. (2004) Multiple evidence for nucleotide metabolism in the chloroplast thylakoid lumen, *Proc. Natl. Acad. Sci. U.S.A. 101*, 1409−1414.
12. Ferreira, K., Iverson, T., Maghlaoui, K., Barber, J., and Iwata, S. (2004) Architecture of the photosynthetic oxygen-evolving center, *Science 303*, 1831−1838.
13. Enami, I., Kikuchi, S., Fukuda, T., Ohta, H., and Shen, J. (1998) Binding and functional properties of four extrinsic proteins of photosystem II from a red alga, *Cyanidium caldarium*, as studied by release−Reconstitution experiments, *Biochemistry 37*, 2787−2793.
14. Popelkova, H., Im, M., and Yocum, C. (2003) Binding of manganese stabilizing protein to photosystem II: Identification of essential N-terminal threonine residues and domains that prevent nonspecific binding, *Biochemistry 42*, 6193−6200.
15. Enami, I., Kamo, M., Ohta, H., Takahashi, S., Miura, T., Kusayanagi, M., Tanabe, S., Kamei, A., Motoki, A., Hirano, M., Tomo, T., and Satoh, K. (1998) Intramolecular cross-linking of the extrinsic 33-kDa protein leads to loss of oxygen evolution but not its ability of binding to photosystem II and stabilization of the manganese cluster, *J. Biol. Chem. 273*, 4629−4634.
16. Shutova, T., Deikus, G., Irrgang, K., Klimov, V., and Renger, G. (2001) Origin and properties of fluorescence emission from the extrinsic 33 kDa manganese stabilizing protein of higher plant water oxidizing complex, *Biochim. Biophys. Acta 1504*, 371−378.
17. Tanaka, S., Kawata, Y., Wada, K., and Hamaguchi, K. (1989) Extrinsic 33-kDa protein of spinach oxygen-evolving complex−Kinetic studies of folding and disulfide reduction, *Biochemistry 28*, 7188−7193.
18. Betts, S., Ross, J., Hall, K., Pichersky, E., and Yocum, C. (1996) Functional reconstitution of photosystem II with recombinant manganese-stabilizing proteins containing mutations that remove the disulfide bridge, *Biochim. Biophys. Acta 1274*, 135−142.
19. De Las Rivas, J., and Barber, J. (2004) Analysis of the structure of the PsbO protein and its implications, *Photosynth. Res. 81*, 329−343.
20. Nowaczyk, M., Berghaus, C., Stoll, R., and Rogner, M. (2004) Preliminary structural characterisation of the 33 kDa protein (PsbO) in solution studied by site-directed mutagenesis and NMR spectroscopy, *Phys. Chem. Chem. Phys. 6*, 4878−4881.
21. Kramer, D., Cruz, J., and Kanazawa, A. (2003) Balancing the central roles of the thylakoid proton gradient, *Trends Plant Sci. 8*, 27−32.
22. Virgin, I., Styring, S., and Andersson, B. (1988) Photosystem II disorganization and manganese release after photoinhibition of isolated spinach thylakoid mambranes, *FEBS Lett. 233*, 408−412.
23. Rutherford, A., and Faller, P. (2001) The heart of photosynthesis in glorious 3D, *Trends Biochem. Sci. 26*, 341−344.
24. Shutova, T., Irrgang, K., Shubin, V., Klimov, V., and Renger, G. (1997) Analysis of pH-induced structural changes of the isolated extrinsic 33 kDa protein of photosystem II, *Biochemistry 36*, 6350−6358.
25. Shutova, T., Khristin, M., Opanasenko, V., Ananyev, G., and Klimov, V. (1992) Proton−acceptor properties of the water-soluble 33-kDa protein from spinach photosystem II, *Biol. Membr. 9*, 836−844.
26. Weng, J., Tan, C., Shen, J., Yu, Y., Zeng, X., Xu, C., and Ruan, K. (2004) pH-induced conformational changes in the soluble manganese-stabilizing protein of photosystem II, *Biochemistry 43*, 4855−4861.
27. Zhang, L., Liang, H., Wang, J., Li, W., and Yu, T. (1996) Fluorescence and Fourier transform infrared spectroscopic studies on the role of disulfide bond in the calcium binding in the 33 kDa protein of photosystem II, *Photosynth. Res. 48*, 379−384.
28. Heredia, P., and De Las Rivas, J. (2003) Calcium-dependent conformational change and thermal stability of the isolated PsbO protein detected by FTIR spectroscopy, *Biochemistry 42*, 11831−11838.
29. Kruk, J., Burda, K., Jemiola-Rzeminska, M., and Strzalka, K. (2003) The 33 kDa protein of photosystem II is a low-affinity calcium- and lanthanide-binding protein, *Biochemistry 42*, 14862−14867.
30. Loll, B., Gerold, G., Slowik, D., Voelter, W., Jung, C., Saenger, W., and Irrgang, K. D. (2005) Thermostability and $Ca^{2+}$ binding properties of wild type and heterologously expressed psbO protein from cyanobacterial photosystem II, *Biochemistry 44*, 4691−4698.
31. Wales, R., Newman, B., Pappin, D., and Gray, J. (1989) The extrinsic 33 kDa polypeptide of the oxygen-evolving complex of photosystem II is a putative calcium-binding protein and is encoded by a multi-gene family in pea, *Plant Mol. Biol. 12*, 439−451.
32. Berthold, D. A., Babcock, G. T., Yocum, C. F. (1981) A highly resolved, oxygen-evolving photosystem II preparations from spinach thylakoid membranes. EPR and electron-transport properties, *FEBS Lett. 134*, 231−234.
33. Laemmli, U. K. (1970) Cleavage of structural proteins during the assembly of the head of bacteriophage T4, *Nature 227*, 680−685.
34. Oakley, G. A., Jones, D. E., Harrison, J. A., and Wade, G. E. (1980) A new method of obtaining arterial blood samples from cattle, *Vet. Res. 106*, 460.
35. Eaton-Rye, J. J., and Murata, N. (1989) Evidence that the amino-terminus of the 33 kDa extrinsic protein is required for binding to the photosystem II complex, *Biochim. Biophys. Acta 977*, 219−226.
36. Permyakov, E. A., Burstein, E. A., Sawada, Y., and Yamazaki, I. (1977) Luminescence of phenylalanine residues in superoxide dismutase from green pea, *Biochim. Biophys. Acta 491*, 149−154.
37. Gribenko, A., and Makhatadze, G. (1998) Oligomerization and divalent ion binding properties of the S100P protein: A $Ca^{2+}$/$Mg^{2+}$-switch model, *J. Mol. Biol. 283*, 679−694.
38. Shutova, T., Villarejo, A., Zietz, B., Klimov, V., Gillbro, T., Samuelsson, G., and Renger, G. (2003) Comparative studies on the properties of the extrinsic manganese-stabilizing protein from higher plants and of a synthetic peptide of its C-terminus, *Biochim. Biophys. Acta 1604*, 95−104.
39. Shutova, T., Irrgang, K., Klimov, V., and Renger, G. (2000) Is the manganese stabilizing 33 kDa protein of photosystem II

attaining a "natively unfolded" or "molten globule" structure in solution? *FEBS Lett. 467*, 137−140.
40. Permyakov, E., Reyzer, I., and Berliner, L. (1993) Effects of $Zn^{II}$ on galactosyltransferase activity, *J. Protein Chem. 12*, 633−638.
41. Oliveberg, M., Vuilleumier, S., and Fersht, A. (1994) Thermodynamic study of the acid denaturation of barnase and its dependence on ionic-strength—Evidence for residual electrostatic interactions in the acid/thermally denatured state, *Biochemistry 33*, 8826−8832.
42. Lydakis-Simantiris, N., Hutchison, R., Betts, S., Barry, B., and Yocum, C. (1999) Manganese stabilizing protein of photosystem II is a thermostable, natively unfolded polypeptide, *Biochemistry 38*, 404−414.
43. Semisotnov, G., Rodionova, N., Razgulyaev, O., Uversky, V., Gripas, A., and Gilmanshin, R. (1991) Study of the molten globule intermediate state in protein folding by a hydrophobic fluorescent-probe, *Biopolymers 31*, 119−128.
44. Permyakov, E. A., Yarmolenko, V. V., Kalinichenko, L. P., Morozova, L. A., and Burstein, E. A. (1981) Calcium binding to α-lactalbumin: Structural rearrangement and association constant evaluation by means of intrinsic protein fluorescence changes, *Biochem. Biophys. Res. Commun. 100*, 191−197.
45. Sonoyama, M., Motoki, A., Okamoto, G., Hirano, M., Ishida, H., and Katoh, S. (1996) Secondary structure and thermostability of the photosystem II manganese-stabilizing protein of the thermophilic cyanobacterium *Synechococcus elongatus*, *Biochim. Biophys. Acta 1297*, 167−170.
46. Veprintsev, D. B., Permyakov, S. E., Permyakov, E. A., Rogov, V. V., Cawthern, K. M., and Berliner, L. J. (1997) Cooperative thermal transitions of bovine and human apo-α-lactalbumins: Evidence for a new intermediate state, *FEBS Lett. 412*, 625−628.
47. Oberg, K. A., Ruysschaert, J. M., and Goormaghtigh, E. (2004) The optimization of protein secondary structure determination with infrared and circular dichroism spectra, *Eur. J. Biochem. 271*, 2937−2948.
48. Ellis, R. (2001) Macromolecular crowding: An important but neglected aspect of the intracellular environment, *Curr. Opin. Struct. Biol. 11*, 114−119.
49. Ellis, R. (2001) Macromolecular crowding: Obvious but underappreciated, *Trends Biochem. Sci. 26*, 597−604.
50. Berggard, T., Silow, M., Thulin, E., and Linse, S. (2000) $Ca^{2+}$- and $H^{+}$-dependent conformational changes of calbindin D(28k), *Biochemistry 39*, 6864−6873.
51. Hutchison, R., Betts, S., Yocum, C., and Barry, B. (1998) Conformational changes in the extrinsic manganese stabilizing protein can occur upon binding to the photosystem II reaction center: An isotope editing and FT-IR study, *Biochemistry 37*, 5643−5653.
52. Hutchison, R., Steenhuis, J., Yocum, C., Razeghifard, M., and Barry, B. (1999) Deprotonation of the 33-kDa, extrinsic, manganese-stabilizing subunit accompanies photooxidation of manganese in photosystem II, *J. Biol. Chem. 274*, 31987−31995.
53. Hillier, W., and Wydrzynski, T. (2000) The affinities for the two substrate water binding sites in the O-2 evolving complex of photosystem II vary independently during S-state turnover, *Biochemistry 39*, 4399−4405.
54. Schwede, T., Kopp, J., Guex, N., and Peitsch, M. C. (2003) SWISS-MODEL: An automated protein homology-modeling server, *Nucleic Acids Res. 31*, 3381−3385.

BI0512750